

# An approach to implement Photovoltaic Self-Consumption and Ramp-Rate Control Algorithm with a Day-to-Day Forecast battery charging, using a Vanadium Redox Flow Battery

Ana Foles<sup>a,b,1</sup>, Luís Fialho<sup>a,b,2</sup>, Manuel Collares-Pereira<sup>a,b,3</sup>, Pedro Horta<sup>a,b,4</sup>

<sup>a</sup>Renewable Energies Chair, University of Évora. Pólo da Mitra da Universidade de Évora, Edifício Ário Lobo de Azevedo, 7000-083 Nossa Senhora da Tourega, Portugal

<sup>b</sup>Institute of Earth Sciences, University of Évora, Rua Romão Ramalho, 7000-671, Évora, Portugal

<sup>1</sup>[anafoles@uevora.pt](mailto:anafoles@uevora.pt)

<sup>2</sup>[lafialho@uevora.pt](mailto:lafialho@uevora.pt)

<sup>3</sup>[collarespereira@uevora.pt](mailto:collarespereira@uevora.pt)

<sup>4</sup>[phorta@uevora.pt](mailto:phorta@uevora.pt)

---

- The authors have no competing interests to declare

- Colour should be used for any figures in print

## Nomenclature

### *Abbreviation, Definition*

API	Application Programming Interface
BAPV	Building Applied Photovoltaics
BCR	Battery charge ratio
BESS	Battery energy storage system
CRR	Controlled ramps ratio
DSO	Distributor System Operator
EG	Energy from the grid
EMS	Energy management strategy
FBU	Overall from battery use
FGU	Overall from grid use
GRF	Grid relief factor
HV	High voltage
MA	Moving average
OBU	Overall battery use
RR	Ramp rate (%/min per nameplate capacity)
SCM	Self-consumption maximization
SCM+RR	Self-consumption maximization with ramp-rate control
SCM+RR+WF	Self-consumption maximization with ramp-rate control with weather forecast battery charging
SCR	Self-consumption ratio
SoC	State of charge (%)
SSR	Self-sufficiency ratio
TBU	Overall to battery use
TGU	Overall to grid use
TSO	Transmission System Operator
VRE	Variable renewable energy
VRFB	Vanadium redox flow battery

## Abstract

The variability of the solar resource is mainly caused by cloud passing, causing rapid power fluctuations on the output of photovoltaic (PV) systems. The fluctuations can negatively impact the electric grid, and smoothing techniques can be used as attempts to correct it. However, the integration of a PV+storage to deal with the extreme power ramps at a domestic/services scale is not explored in the literature, neither its effective combination with other energy management strategies (EMSs). This work is focused on using a battery energy storage unit to control the power output of the PV system, maintaining the ramp rate (RR) within a non-violation limit and within a battery state of charge (SoC) range, appropriate to perform this RR management at the domestic/services scale. For this purpose, the authors explore the vanadium redox flow battery (VRFB) technology. Based on model simulation, key-performance indicators (KPI) are studied and improved, and finally, experimental validation is carried out. A comparison among three EMSs is made: a self-consumption maximization (SCM), a SCM with ramp-rate control (SCM+RR), and the last strategy performing also night battery charging based on the day ahead weather forecast (SCM+RR+WF). The weather forecast allowed the battery SoC control, preparing it to carry out the RR control the next day. The results show that SCM+RR+WF, especially in wintertime, is an excellent approach to manage PV+battery systems. This strategy successfully controlled 100% of the violating power ramps, obtaining also a self-consumption ratio (SCR) of 59%, and a grid-relief factor (GRF) of 61%.

**Keywords:** PV solar energy; energy storage; self-consumption; ramp rate; VRFB

## 1. Introduction

At the end of 2019, the global installed renewable capacity reached 2,537 GW, more than 176 GW last year [1]. Wind and solar energy accounted for 90% of the global capacity just added. In 2019, photovoltaic (PV) solar energy had a 3% share in the world generation mix, maintaining a 2050 forecast of 23% [2]. Since there is a significant share of renewable energy, which is variable (VRE), it is necessary to impose limits for its integration into the network [3]. The integration of VRE obeys a regulation that stipulates limits of the allowed electric energy exchanged with the grid, to correspond to the measures of electrical energy quality. The controlled parameters are the voltage and frequency operating ranges, power quality,

reactive power capacity for voltage control, frequency support, fault behaviour, active power gradient limitations, simulation models, active power management, communication, and protection. The network's energy injection ramps, caused by the fluctuation of primary energy from renewable energy (RE) generation, are concerned with the limitations of the active energy gradient. These are generally classified using a minute interval, considering the PV nameplate capacity. The limitation of the ramps contributes to more balanced management of the energy system through the DSO, contributing to increasing the efficiency of the systems. The increase in VRE's contribution in final energy consumption can be resolved by creating a ramp limit, which is already in the legislation of some countries around the world [3].

Countries with a significant number of solar PV installations have limitations in supplying energy to the grid. The ENTSO-E (European Network of Transmission System Operators) requires the RR limit to be specified by regional TSO, if necessary. A deeper analysis of the general grid codes for PV integration can be consulted in [4]. Some of the detailed active power limitation regulations for VRE currently established for several countries are highlighted in the following. Germany follows a regulation that states that for PV generators under 30 kW, which cannot be remotely controlled, a feed-in limitation of 70 % of the system's peak power is needed. If the installed capacity is greater than 1 MVA, the RR limit is 10% of the rated power per minute. Concerning wind energy, if generators trip due to grid fault or frequency, the RR is limited to go back online, from 10-20% of rated power per minute. In 2012, Puerto Rico island developed the Puerto Rico Electric Power Authority (PREPA) regulation, imposing a 10% nameplate capacity per minute as a RR limitation of grid injection [5]. In Denmark, the wind power plants connected to a high voltage grid (HV) have no constraints on active power gradients, although the generators must be able to constraint their RR if demanded by the grid operator [3]. Also, a maximum ramp-rate of 100 kW/s is required [6]. Ireland developed the EirGrid Plc regulation, where it is established that the wind farm power stations must be able to control the RR of its active power output over a range of 1-100% of its nominal capacity per minute. The wind turbines must be able to restrict ramping [3]. Also, it has a positive ramp-up limit of 30 MW per minute. In the Philippines, it is required to limit active power during over-frequency. The largest plants must be able to limit ramps. Finally, in China, the National Standard for the maximum ramp range of PV power stations must be less than 10% of the installed capacity per minute [4].

Short-term energy fluctuations are directly related to the area of the PV plant and its geographical dispersion, and for this reason, in general, the small area, associated with a domestic/services PV installation, becomes especially subject to severe fluctuations in PV energy [7]. The RR limitation can be achieved through three main techniques, namely, operation of the PV system below its nominal capacity, bypassing the MPP [8], or through the use of a Battery Energy Storage System (BESS) to absorb or inject the excess of generated PV energy when the ramp limit is violated [9]. Smoothing methods are mainly divided into two categories: filter methods and gradient methods. For more information about the methods used, the study carried out in [6] presents the comparison of different ramp smoothing filter techniques, using a BESS. RR limitations are generally studied in large PV installations, where their effects are more noticeable, due to the reduction or sudden increases in the power injected into the grid. Several studies approach the RR control, although there is a clear lack of studies devoted to the domestic and services sectors. In this work, the authors focus on the Moving average (MA) filter type, which is considered the most traditional filter technique, although it is also mentioned that it can lead to increased battery cycling. This is also the reason why the present study was chosen to apply the MA filter to a VRFB. This BESS technology, although a battery with moderate energy density, allows (if necessary) a high number of cycles without significantly reducing its performance, capacity, or life. The time frame for applying the MA technique is a very important issue and must be carefully chosen. In [10] the study of the author is done considering a time interval of 15 minutes. In [6] the authors explore time intervals of 2.5, 5, 7.5, and 10 minutes, evaluating the number of fluctuations and their impact on the application of the technique. The study developed in [10] shows that a shorter period results in a larger number of successfully controlled ramps. Taking into account this conclusion, and the technical limits of our micro-network, for the MA, a period of 20s was chosen. More details are presented in the next section.

PV for self-consumption is the most studied and applied strategy to operate a PV system with or without a battery (depending on the consumption needs). In the context of the legislation in force, the DL 169/2019, PV self-consumption is highly promoted, being a starting point of this work. In this topic, a greater volume of works has been developed, using a BESS. A brief highlight is given to the work developed in [11], with an SCM real-time implementation on the VRFB of the University of Évora (UÉvora), and the study in [12] where not only the PV self-consumption is studied, but also the PV generation forecast, using the Germany-specific grid feed-in limitations, to relieve the grid from fluctuations. In this

work, the exploitation of the conjunction of the SCM and the RR control is a novelty, both in simulation, as well as in the application.

### **1.1. Structure of the work**

Section 1.2 of this work presents and describes the EMSs used in this paper. Section 1.3 presents a preliminary assessment made for the historical generation data of the PV system on-site, allowing to quantify and characterize the ramp rate occurrence, taking into account the legal limits referred.

Section 2 presents the work's overall methodology, starting with the description of the microgrid architecture and setup, as well as the vanadium battery model, used to describe the VRFB behaviour. Section 2.2 presents the PV generation and load profiles used for the EMSs simulations, corresponding to typical data of the Portuguese domestic/services sector. One of the novelties of this work was to base the decision of night charge on the use of a weather forecast, making the best energy use of the battery (Section 2.3). The next section (2.4) shows the RR definition used, and the calculation method implemented. The effectiveness of the RR control algorithm is only achieved through a wise choice on the time frame of the EMS (discussed in Section 2.4). In order to assess and compare the EMS simulation results, Key Performance Indicators (KPI) were defined and used, as depicted in Section 2.6.

Section 3 presents the simulation development of the EMSs, implemented on the MATLAB software. The simulation algorithms are showed in a flowchart form and detailly explained.

Section 4 shows the simulation results for the 3 EMSs, comparing the resulting KPIs and SoC control results.

The second phase of this work was to implement the SCR+RR+WF strategy with real operating conditions, in order to validate the strategy performance and compare its results to the simulation. This EMS was implemented in LabView software and Section 5 presents the experimental validation results.

Section 6 presents the discussion of the overall results, both from the strategy simulation phase and from the experimental validation of the third strategy.

Finally, some conclusions about this work and its results are presented in Section 7.

## 1.2. PV+battery energy management strategies

In this section, the three energy management strategies used in this work are presented. The self-consumption maximization (SCM – strategy 1) is a very simple strategy which maximizes the usage of the PV generation throughout the day. The user installation can benefit from having a BESS to increase the PV power self-consumption. This strategy is usually the most common in industry and residential solutions, due to its simple application and improved match with the load demand.

The second strategy is the self-consumption maximization with ramp-rate control (SCM+RR – strategy 2). As previously discussed, the continuous increase of PV systems worldwide has consequences for the management of the electric public grid, mainly due to its intermittency and variability characteristics, probably requiring imposing limits, e.g., to the power ramps produced by the PV systems. The control of power ramps can be achieved with the use of BESS, slightly impairing the self-consumption maximization results. In this case, the self-consumption is carried out, although when the ramp rate limit is violated, the battery unit is used primarily to control the ramp. The ramp rate is calculated as a percentage per minute over the nominal PV power. When a violation of a pre-set RR limit occurs, and the battery presents suitable capacity (within the allowed SoC range) and power, the RR algorithm is activated: the battery absorbs the surplus PV power, or injects power in order to control the power ramp rate. When there is no violation of the ramp limits, the PV self-consumption maximization strategy is used. In this strategy, a SoC control is not carried out.

The third strategy studied in this work is a Self-consumption maximization with Ramp-rate control and a battery charging based on a weather forecast (SCM+RR+BCF – strategy 3). A ramp control is a concurrent objective with the maximization of self-consumption regarding the use of the battery. In the average load curve characteristic of a domestic or services installation, a peak consumption at the end of the day often occurs after sunset or at night. Supplying this night-time consumption, to maximize PV self-consumption, has the consequence of the battery SoC reaching the next morning close to its minimum limit. Similarly, a summer day with high solar radiation and clean sky, and/or low energy consumption in the user installation, can charge the battery up to its upper limit of SoC. Due to the Power-SoC characteristics of the BESS technologies (e.g., lithium-ion, vanadium redox flow, sodium-nickel chloride, among others), the available power to charge/discharge is severely constrained near the upper and lower SoC limits, respectively. These available power technical restrictions hinder the full control of power ramps. As a way to overcome this, a

SoC control is implemented, through a battery charge-discharge command target conditioned to the site weather forecast for the next 12h. The meteorological forecast categories that indicate high probability of the power ramps occurrence were selected. More details about this method are presented in section 2.5. This control technique allows that, if the forecast indicates, the battery will start the next day with its SoC close to 50 %, range where it presents its maximum power available to perform the control of extreme power ramps.

### 1.3. A variability analysis of the solar PV data of the UÉvora systems

The RR is a measure which should not be observed through a quantitative-only analysis, since its negative impact is related to matters like the extension of household appliances lifetime, and to contribute to the grid stability, helping the DSOs and TSOs. As an example, a calculation was made for the RR, for 1-minute period, for the nameplate capacity of one of the UÉvora Building Applied PV (BAPV) systems, with one year of PV recorded data, shown in Figure 1.



Figure 1 - Rooftop PV system with 6740 W installed power, in one of the UÉvora's microgrids.

The nominal power of the BAPV installation is 6740 W, and its monitoring data is collected through an in-house developed software, using the LabVIEW environment. The control is conducted in a 2 second time frame, collecting data from a precision power analyser (Circutor CVM-1D [13]) and the PV inverter. The data was compiled in 1-minute samples, and the RR was calculated for the entire year of 2018. The RR results are shown below, in Table 1.

Table 1 - RR in %/min of the nameplate capacity of the PV system (UÉvora, 2018 data).

RR (%/min) in the year of 2018	Percentage of total RR in one year (%)
< 5 %/min	78.47
≥ 5 %/min	8.090
≥10 %/min	5.161
> 10 %/min	4.833
≥ 50 %/min	0.650

From the observation of Table 1, almost 79% of the RRs presents low values (lower than 5%/min of the PV nameplate capacity), which is an expected result, given the PV installation size. These RR values have probably low or no impact on the grid. The value of RRs of 5% and 10% were used as references, being the representative values currently present in the grid-codes previously presented. For the year 2018, RRs higher or equal to 10 %/min of the PV installation's nameplate capacity, occurred in 5% of the ramps, giving, in this situation, a quantitative reference of the number of ramps that should be controlled. To increase the degree of confidence of these results, a substantially greater data period is required, ideally, several years. The existence of systems with monitoring of long-term PV generation data with high frequency (as, for instance, data logging at 2s) is rare and should be an effort to be implemented in the future of experimental installations.

The results of Table 1 are representative of the location and specifications (tilt, azimuth, among others) of this single PV system, due to the direct relationship between this solar radiation data and the occurrence of power ramps, as the analysis of the solar radiation meteorological data.

## 2. Methodology

### 2.1. UÉvora microgrid and VRFB modelling

The VRFB (60/5 kWh/kW) is integrated in a microgrid, presented in Figure 2, which is currently exclusively devoted for the systems operation study, and integration with the building at a real scale. This microgrid is equipped with a PV system with 3.5 kWp of polycrystalline technology, and 3.2 kWp of monocrystalline technology, precision monitoring equipment and a control system.



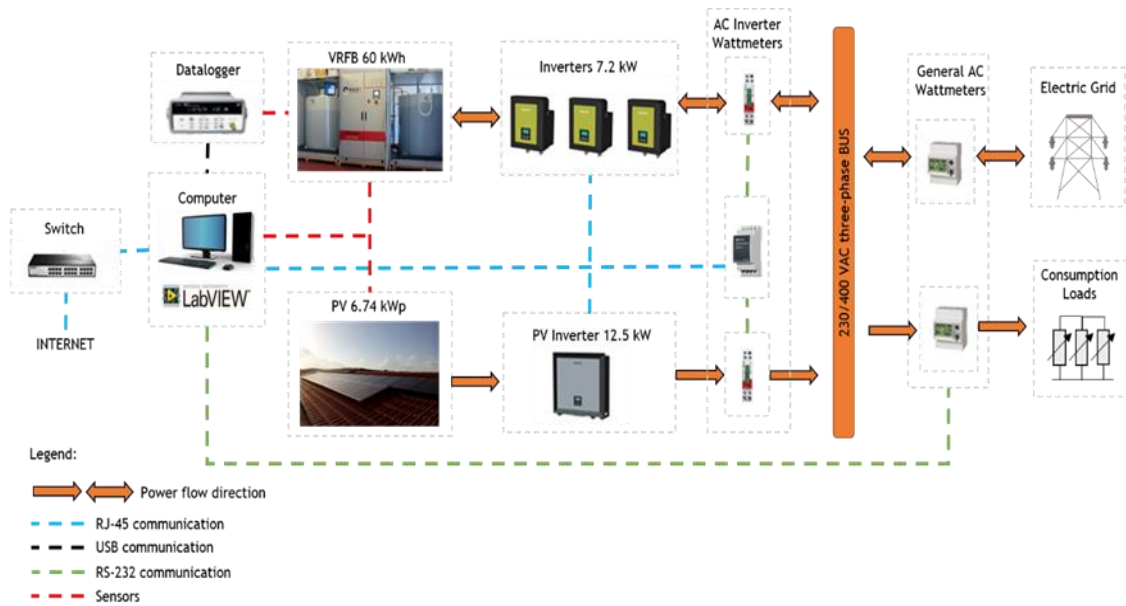


Figure 2 – Schematic of UÉvora's VRFB microgrid equipment's connection and energy fluxes.

The VRFB has two electrolyte tanks, two pumps that allow the electrolyte to flow, and a stack: the energy conversion unit. The stack is a dynamic system, and its performance depends on multiple effects: electrochemical, fluid dynamics, electric and thermal. Different oxidation states of dissolved vanadium ions in the electrolyte ( $V^{2+}$ ,  $V^{3+}$ ,  $V^{4+}$ ,  $V^{5+}$ ) store or deliver electric energy through a reversible chemical reaction. This VRFB was the object of study in previous works, and the most recent include the battery full electrical modelling, developed, and validated on a real scale, considering its general operating conditions. This model is fully detailed in the research conducted in [15]. As example of the modelling performance results, Figure 3 shows the VRFB's stack voltage comparison among the operation data and the modelling simulation results developed in MATLAB software.

Considering the small relative error of the model when calculating the battery key-parameters, including the SoC, and the availability of power (charge/discharge), a battery operating range of 20% and 70% of SoC was selected. The VRFB model [15], was implemented and used in all the control algorithms and energy management strategies. The use of this validated battery model helps the control implementation with the smallest possible error.

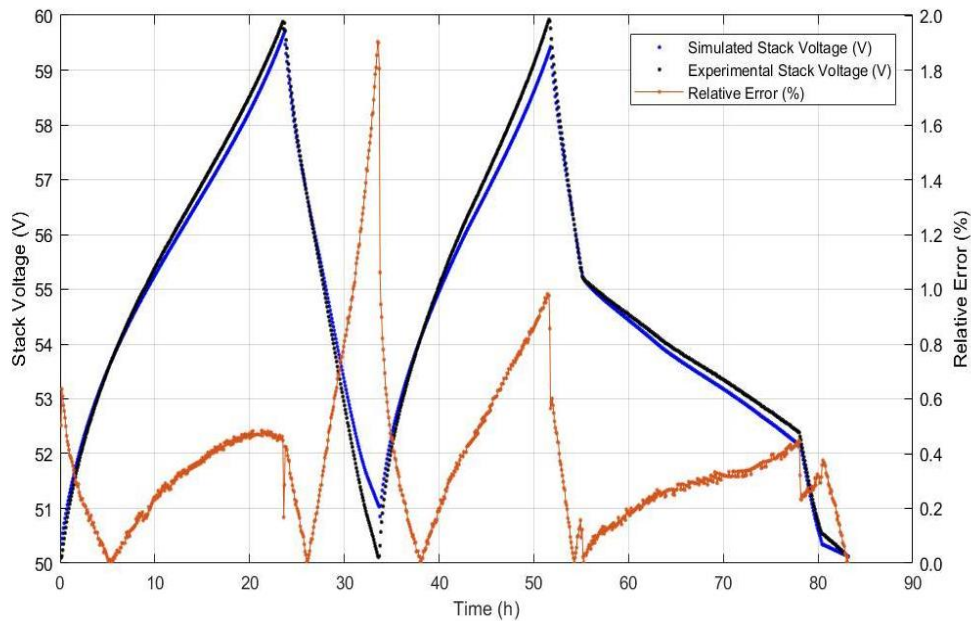
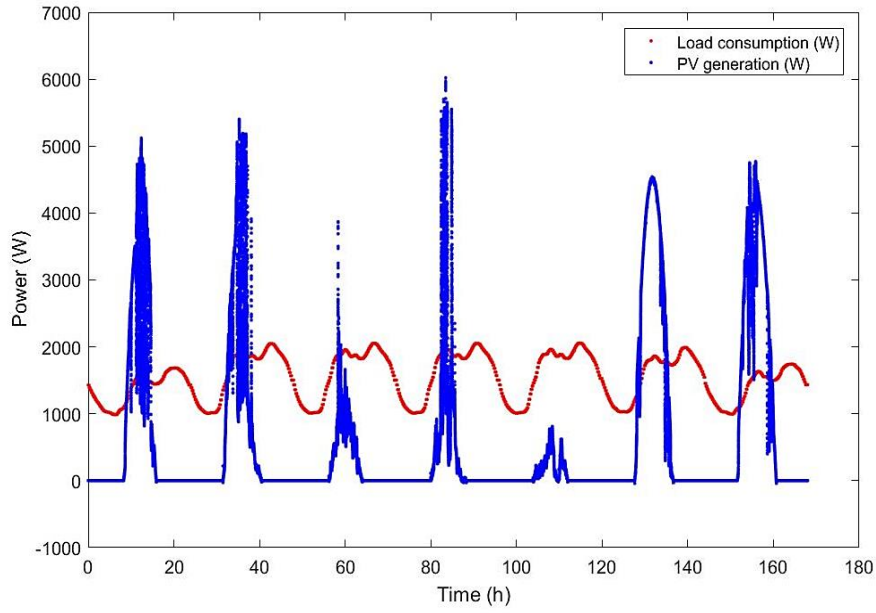


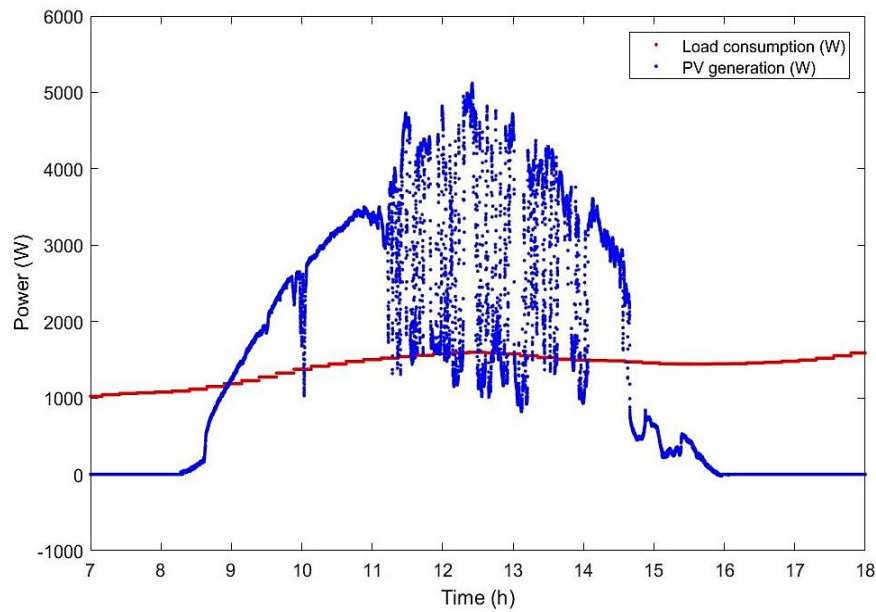
Figure 3 - Voltage of the VRFB's stack, experimentally obtained and compared with the simulated values, with a maximum relative error under 2%, with SoC range of 5% to 90%.

## 2.2. PV-generation and load profile data

The PV profile corresponds to the data obtained with the UÉvora's PV system (Figure 1), during one week from 1<sup>st</sup> to the 7<sup>th</sup> day of January of 2018, with a 2 second intervals data logging. The load profile used is made available by EDP Distribuição – Portuguese DSO company – with 15 minutes average load data for the year of 2018 [14]. This data was previously treated, with the help of the MATLAB software, in the way of corresponding to the PV data sampled time frame. The used data can be seen below, in Figure 4, where a) presents the collected data, PV and load profiles, for the first seven days of January of 2018, and b) for a single day of January, the 1<sup>st</sup>.



a)



b)

Figure 4 – Solar PV profile and load profile considered in this study for a) 1 week of January, from day 1 to day 7 of 2018; b) the 1st of January of 2018.

### 2.3. Battery charging with weather forecast

In strategy 3, SCM+RR+BCF, the battery will be charged to values near the 50 % SoC when needed, with data input from weather forecast (ramp-rate occurrence), using data

forecast produced by IPMA (*Instituto Português do Mar e da Atmosfera*). IPMA is a Portuguese public body, which is responsible for, among other many tasks, forecasting the states of the weather and sea, for all necessary needs. The forecasted data, associated with the location of the geographical and seismic events, are made available in their Application Programming Interface (API) in a JSON format [16]. The data is obtained automatically through a forecast statistic process with forecasts of two numerical models – ECMWF [17] and AROME [18]. These forecasts are updated two times per day, at 00 UTC (available at 10 am) and 12 UTC (available at 8 pm). In the summertime, the Portuguese legal hour is UTC+1, and in the wintertime, the legal hour is equal to UTC. In the referred online API, daily meteorological data forecast up to 5 consecutive days by region can be found, and daily meteorological data forecast up to 3 consecutive days, with aggregated information per day. Each Portuguese region has a global code id, which identifies it. Every twelve hours, the forecast information on the website is updated, for each region. IPMA forecasts roughly 41 regions, both onshore and offshore. The website makes available the following days' weather indicators: precipitation probability (no precipitation, weak, moderate, or strong), minimum and maximum temperatures in °C, wind direction (N, NE, E, SE, S, SW, W, NW), id weather type (0 to 27 weather description states), wind speed class (weak, moderate, strong, very strong). In this work, relevance was given to the id weather type, for which a number is attributed, corresponding to a weather description. This description can be observed in Table 2.

Table 2 – IPMA API ID weather type correspondence map [16]. The bold values correspond to the ones used for the 50 % battery SoC target.

Number	Correspondence	Number	Correspondence
---	-99	<b>14</b>	<b><i>Intermittent heavy rain</i></b>
0	No information	15	Drizzle
1	Clear sky	<b>16</b>	<b><i>Mist</i></b>
2	Partly cloudy	<b>17</b>	<b><i>Fog</i></b>
3	Sunny intervals	18	Snow
<b>4</b>	<b><i>Cloudy</i></b>	19	Thunderstorms
<b>5</b>	<b><i>Cloudy (High cloud)</i></b>	20	Showers and thunderstorms
6	Showers	21	Hail
7	Light showers	22	Frost
<b>8</b>	<b><i>Heavy showers</i></b>	<b>23</b>	<b><i>Rain and thunderstorms</i></b>
9	Rain	<b>24</b>	<b><i>Convective clouds</i></b>
10	Light rain	<b>25</b>	<b><i>Partly cloudy</i></b>

11	<i>Heavy rain</i>	26	<i>Fog</i>
12	Intermittent rain	27	<i>Cloudy</i>
13	Intermittent light rain		

---

In this work, the selected relevant information periodically obtained is the latest information per region, regarding the weather forecast for the following day. With the help of this information, the battery SoC is prepared for the next day, as needed. The preparation is made through battery charging during the night hours (in general there is very low energy consumption from domestic users during those hours), and for that reason, this control type is optimal for the Portuguese bi-hourly and tri-hourly household tariffs, with lower electricity price during the night [19]. Every day at 1:30 am, the algorithm consults the IPMA API looking for the “idWeatherType” number correspondence, to know if it should act on the power command of the battery. The command will be a charging-only command, since it is expected that the battery at the end of the day, to be near its lowest SoC (limit), given the load profiles used. If none of the conditions is satisfied (near lowest limit SoC, or “bad” weather day), the SoC of the VRFB will be only dependent on the PV self-consumption objective.

#### 2.4. Ramp rate calculus with MA method

In general, the classic way of representing the RR is defined as  $RR_{classic}$ , as presented in Eq. (1),

$$RR = \frac{P_{PV}(t) - P_{PV}(t - \Delta t_R)}{\frac{P_N}{\Delta t_R}} \times 100 \quad (1)$$

where,  $P_{PV}$  – PV power (W) and  $t - \Delta t_R$  – Time differential of the RR, typically equal to the unit (min).

The MA was used in this study as the power smoothing technique for the reasons mentioned previously. At each iteration, the calculated RR is defined as  $RR_{MA}$ . The difference is that the variable  $P_{PV}(t - \Delta t_R)$  is the average of the PV power defined in the desired interval, in this case, for the previous 20 seconds. This method functions with the averaging of the previous PV measurements, in a chosen period,  $t$ , and the battery command is calculated from Eq. (2) shown below,

$$P_{battery}(t) = \frac{\sum_{i=0}^{w-1} P_{PV}(t) - P_{PV}(t - i)}{w} - P_{PV}(t) \quad (2)$$

For more details regarding the RR calculation, the work made by the authors of [6] should be consulted.

## 2.5. Time frame

The moving averaging time frame is an aspect that should be sensibly weighted. The study developed in [20] research carefully the PV time averages impacts on the small and medium-sized PV installations. The authors conclude that a time frame of 15-minute averages describes these ramps poorly. Because of this concern, an adequate time frame was considered. For the one week of PV data considered in this study, the theoretically controlled ramps were calculated, using the 10%/min RR, with an average of different periods of PV intervals. The obtained values are presented in Table 3. The corresponding PV averaging to these time frames can be observed in Figure 5, presented below.

Table 3 - Controlled ramps for the studied week, over different time frames of PV average values; impact on the controlled ramps.

Time frame	Controlled ramps in the chosen week (RR $\geq$ 10%/min)
2 s (without averaging)	5716
10 s	5751
20 s	5660
30 s	5570
60 s (1 min)	5039
300 s (5 min)	364
600 s (10 min)	0
900 s (15 min)	0

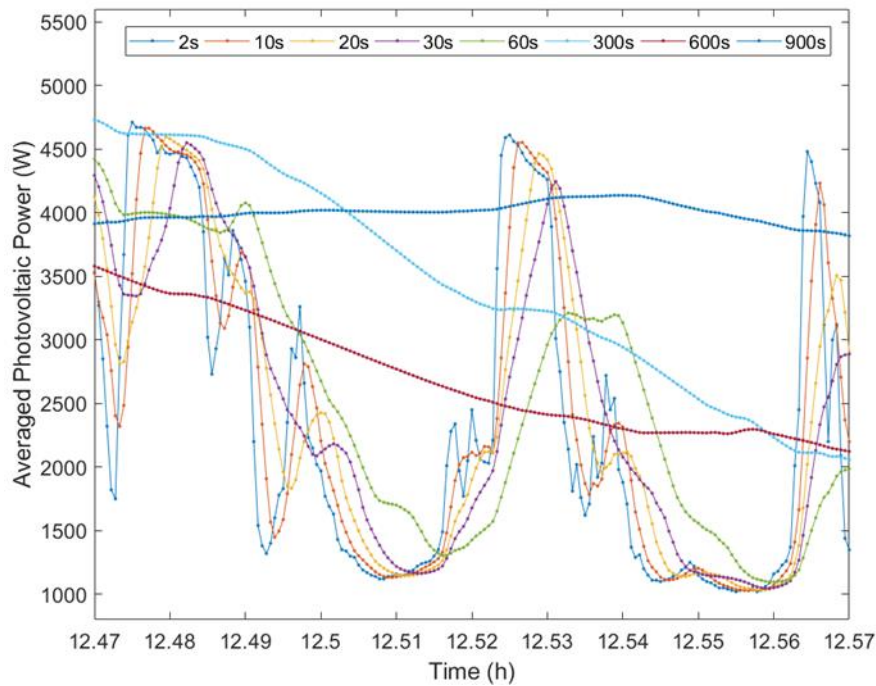


Figure 5 – PV average of the time frames studied and presented in Table 3. The 2s correspond to the raw data extracted from the PV installation under study. The remaining time frames are the PV averaging correspondent to each of that time frame.

The results obtained support the study previously referred [20], for the domestic PV installations, as the average time frame increases, fewer ramps are detected and controlled. Alternatively, if the average time frame is too small, the impact will be short. A sensitivity analysis of this parameter should be made. The simple MA, being simple to implement and with low computational effort, can let through unexpected artifacts such as peaks in the results. In accordance, a time frame of 20 seconds was chosen. This PV averaging time frame can be observed in Figure 6, from the noon (12:00h) to the 14:00h (to be appropriately visible) of the 1<sup>st</sup> of January of 2018.

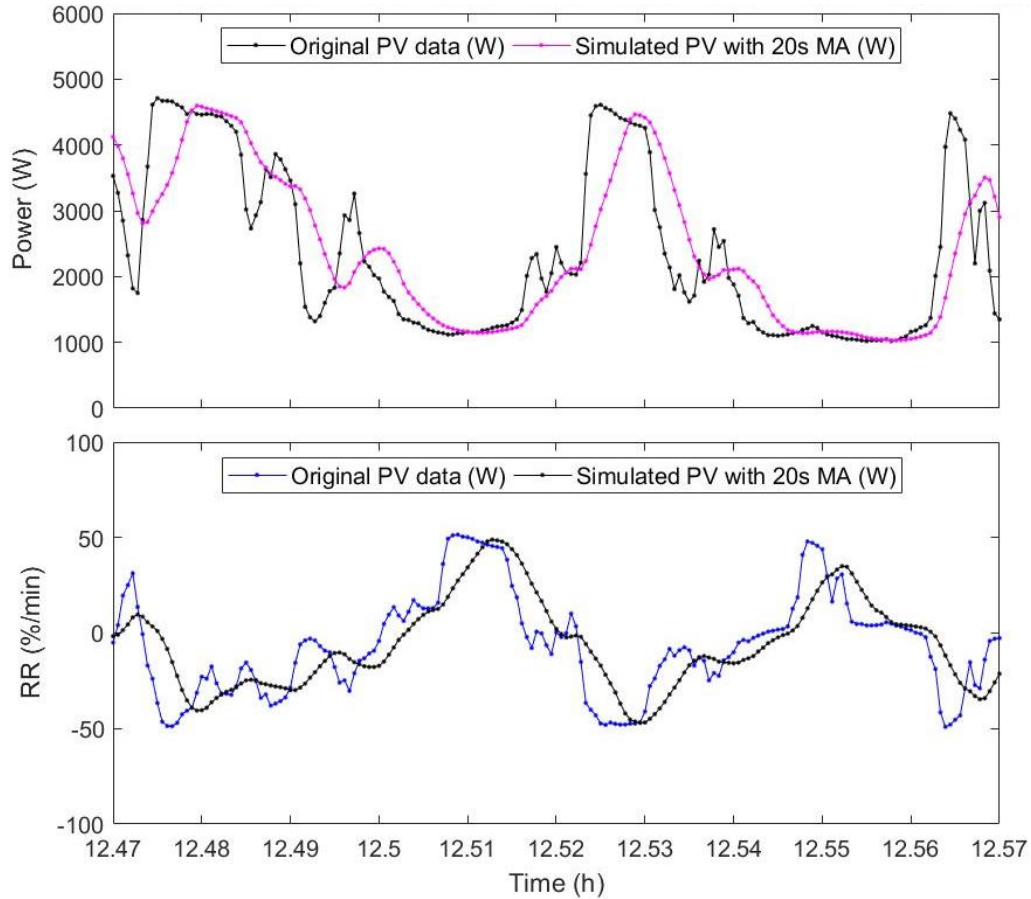


Figure 6 – (Top) PV average with a time frame of 20 seconds, and (Bottom) correspondent Ramp-rate calculus; for the first day of January of 2018, obtained through the 2 s measurement data of the PV system of 6740 W of UÉvora.

## 2.6. Key-performance indicators

To reach a final decision whether to approve or not a determined EMS, a proper method for evaluation should be conducted. To determine the attractiveness of a certain time investment, suited key-performance indicators are calculated. The parameters are based on the sum of the energy used throughout the days of the strategy application. In the following, the indicators are enunciated.

The self-consumption ratio (SCR) is the share of the PV energy consumed by the installation over the total PV energy generated. The PV energy produced can be consumed indirectly by the battery (including losses). The SCR calculation can be expressed as follows in Eq. (3),

$$SCR = \frac{E_{PVconsumed}}{E_{PVgenerated}} \quad (3)$$



where,  $E_{PVconsumed}$  is the PV energy generation consumed directly or indirectly, and  $E_{PVgenerated}$  is the total PV energy generated by the PV installation. The self-sufficiency ratio (SSR) is the share of the consumed PV energy generation over the total consumption needs, as expressed in Eq. (4),

$$SSR = \frac{E_{PVconsumed}}{E_{Load}} = \frac{E_{Load} - E_{Grid}}{E_{Load}} \quad (4)$$

where,  $E_{Load}$  is the total consumption needs, and  $E_{Grid}$  is the injected and extracted energy to/from the grid. The grid-relief factor (GRF) is a measure of the total energy of the installation loads, which is not exchanged with the grid, expressed in Eq. (5).

$$GRF = \frac{E_{Load} - E_{Grid}}{E_{Load}} \quad (5)$$

The overall battery use (OBU) can be described as the amount of energy used to charge and discharge the battery unit, over the installation consumption needs, and is expressed by Eq. (6), following represented,

$$OBU = \frac{E_{charge} + E_{discharge}}{E_{Load}} \quad (6)$$

where,  $E_{charge}$  is the total energy used to charge the battery, and  $E_{discharge}$  the total energy used to discharge the battery. The battery charge ratio (BCR) is the total energy used to charge the battery, over the overall energy sent and received to/by the battery. This expression is represented in Eq. (7),

$$BCR = \frac{E_{charge}}{E_{battery}} \quad (7)$$

where  $E_{battery}$  represents the total energy sent to charge and discharge the battery, in absolute values. The energy from the grid (EG) is the amount of energy extracted from the grid, considering the total energy exchanged with the grid, expressed in Eq. (8),

$$EG = \frac{E_{fromGrid}}{E_{Grid}} \quad (8)$$

where,  $E_{fromGrid}$  is the energy needed to extract from the grid to supply the energy consumption needs, in the overall strategy, and  $E_{Grid}$  the total amount of energy exchanged with the grid. The overall from grid use (FGU) is described by the amount of energy extracted from the grid in the overall installation consumption needs, represented by Eq. (9),

$$FGU = \frac{E_{fromGrid}}{E_{Load}} \quad (9)$$

The overall to grid use (TGU) can be described as the amount of energy injected into the grid, over the overall installation consumption needs, and is expressed in Eq. (10),

$$TGU = \frac{E_{toGrid}}{E_{Load}} \quad (10)$$

where,  $E_{toGrid}$  is the energy sent to the grid. The overall from battery use (FBU) is the amount of energy extracted from the battery in the overall installation load profile, expressed in Eq. (11),

$$FBU = \frac{E_{fromBattery}}{E_{Load}} \quad (11)$$

where,  $E_{fromBattery}$  is the energy used to discharge the battery. The overall to battery use (TBU) can be described as the amount of energy sent to the battery, over the overall installation load profile, represented in Eq. (12),

$$TBU = \frac{E_{toBattery}}{E_{Load}} \quad (12)$$

where,  $E_{toBattery}$  is the energy used to charge the battery. The controlled ramps ratio (CRR) is the rate of the total number of the ramps (up and downs) controlled with the use of the battery using the EMS, over the total number of ramps (up and downs) without the use of an EMS, expressed by Eq. (13),

$$CRR = \frac{Nr_{strategy}}{Nr_{original}} \quad (13)$$

where,  $Nr_{strategy}$  is the total number of ramps controlled using the EMS, and  $Nr_{original}$  the number of ramps that occur without an EMS.

For the reader to be engaged with the key performance indicators, a best-case scenario for the prosumer (self-consumption user/installation owner) point-of-view is presented. This reference value can help the reader to understand how close or distant a strategy is from its ideal (best-case) scenario. The best-case for one indicator could imply the worst case of another. The week chosen in this study can also influence some of the KPIs. The KPI's best-case scenarios are shown in Table 4.

Table 4 - Best case-scenarios of the KPIs, considering the SCM strategy.

KPI	Ideal best value	Direct meaning, from the point of view of the prosumer
SCR	1	The amount of PV energy produced meets with the PV energy consumed
SSR	1	The amount of PV energy consumed meets the energy consumed
GRF	1	Level of independence from the grid, from the user point-of-view (if equal to 1, there is no energy to the grid).
OBU	Battery+PV profiles dependent. Here, 31%.	Level of energy exchanged with the battery (charge/discharge) in the overall profile load (considering PV generation and the studied period).
BCR	Equal to 0.5, with a battery efficiency of 1	Maximum possible energy used to charge the battery. Dependent of the battery energy capacity
EG	1 (should be weighted)	Quantification of the amount of energy coming from the grid or going to the grid. Equal to 1 means the energy sent to the grid is 0.
FGU	0	Equal to 1 means that all the overall consumed energy comes from the grid.
TGU	0	Equal to 1 means that the energy injected into the grid is equal to the load profile.
FBU	1	Equal to 1 means that all the consumed energy comes from the battery.
TBU	0	Equal to 1 means that all the energy sent to the battery (charge) is equal to the load energy needs.
CRR	1	Equal to 1 means all ramps that violate the RR reference are controlled.

### 3. Simulation of the Energy Management Strategies

The three strategies algorithms (SCM, SCM+RR, and SCM+RR+WF) were computed and simulated in a MATLAB environment, with the same input data (load profile, PV generation profile, and VRFB model), to check suitability and feasibility. In a previous study, this VRFB was characterized and modelled, and the optimal conditions were defined, considering the approximated ambient temperature of 25°C [15]. The chosen SoC operating range from 20% to 70%, given the available operational power of charge and discharge. This power considers the relation of available power given the current SoC is considered (Power-SoC), for optimal battery operation. Its nominal energy capacity is 60 kWh, which means it

operates with 30 kWh of its useful capacity (for the chosen SoC range). The maximum power of charge/discharge is 5000 W, the VRFB nominal power. The inverters' energy consumption, in standby mode, of 30 W is considered in the modelling. The three simulations were initiated at a SoC of 50 %, and the EMSs were tested in a frame of one week, with a time frame period of 2 seconds.

The first strategy is a PV SCM with the help of the battery. The PV-generated energy sent to the battery for later consumption has losses accounted for inverters and battery efficiency. In the second strategy, PV self-consumption operates jointly with a ramp control, when a RR limit is violated. In the third strategy, the main difference from the previous is that the battery charges at night if needed (only interesting for bi-hourly and tri hourly tariffs). The charging should reach a value near the SoC setting value as possible, up to a maximum charging duration during the night (i.e., a limit of maximum charging hours at night is imposed). The night battery charging power setpoint was defined to be 2700 W, with a battery SoC target of 50 %. The night charging only happens if the next day's forecast indicates a cloudy day, considering the map developed in Table 2. The cloudy day indicates a higher probability of occurrence of PV power ramps. The flowchart of this algorithm part (part I) is presented in Figure 7. The RR algorithm is activated when its real-time calculated result is equal to or larger than the 10 %/min RR value. Figure 8 presents the algorithm performing RR control, when the RR limit is violated (part II). The SCM algorithm was presented and validated in the work of [11].

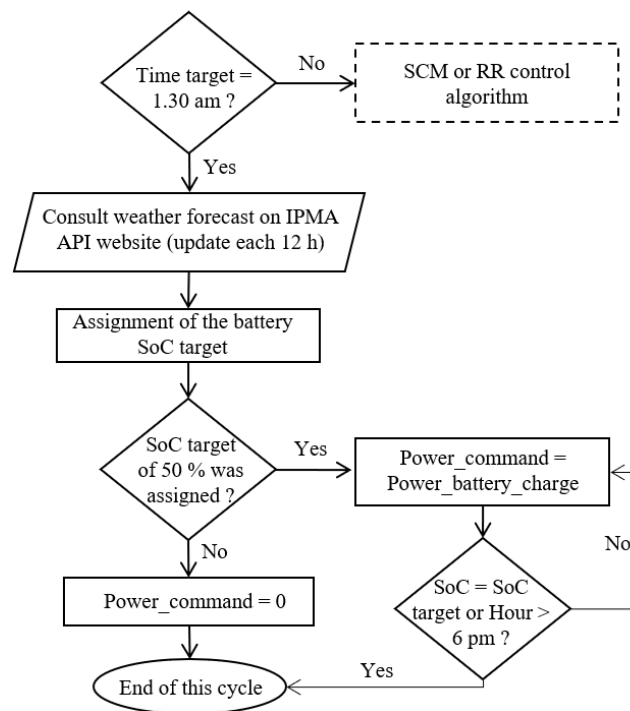


Figure 7 – Algorithm flowchart of the weather forecast with the IPMA API and SoC control.

Legend (Figure 7):

Time\_target – Initial hour for the beginning of the night charge (h).

SoC target – Target to which the SoC should achieve, set as 50 %.

Power\_command – Power command value sent/received to/from the battery (W).

P\_battery\_charge –Constant charge power sent to charge the battery, in nightly hours (W).

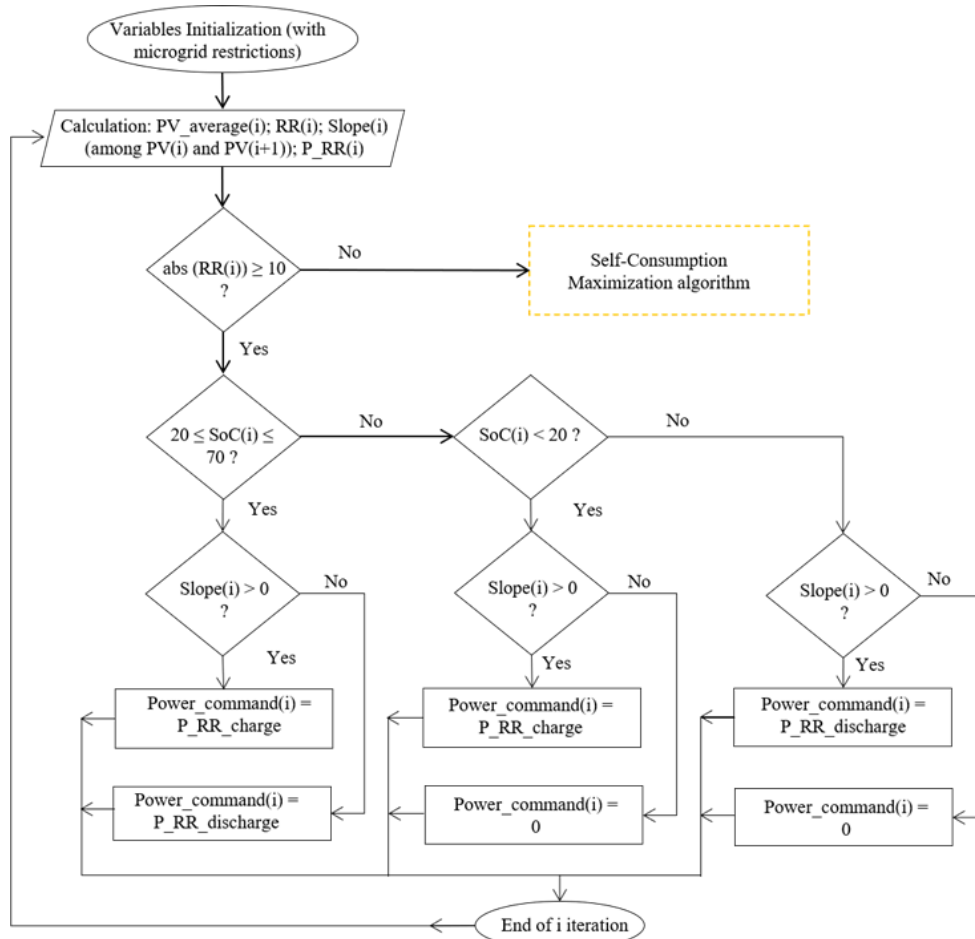


Figure 8 - Ramp-rate control algorithm flowchart, highlighting the battery power command power calculated at each iteration, with a cycle time frame of 2s.

Legend (Figure 8):

i – Cycle iteration number

PV\_average –PV values average of samples correspondent to 20 s (W)

P\_RR – Equivalent to the  $P_{battery}$  of Equation (2) presented in Section 2.4 ( $P_{RR\_charge}$  -  $P_{battery}$  is a battery charge command and  $P_{RR\_discharge}$  -  $P_{battery}$  is a battery discharge command)

Slope –Slope of the two consecutive values of PV

#### 4. Simulation Results

The KPIs were calculated for each of the studied strategies, for one week of January. The results can be observed in Table 5, presented below.

Table 5 - Results of the KPIs, for the studied week of January.

Strategy / Indicators	1 SCM	2 SCM+RR	3 SCM+RR+WF
SCR	58.6	58.7	59.2
SSR	21.8	22.9	21.8
GRF	57.9	63.3	60.8
OBU	31.1	26.4	49.2
BCR	38.7	37.4	40.9
EG	98.8	95.2	94.9
FGU	57.2	60.2	57.7
TGU	0.71	3.06	3.09
FBU	13.2	10.8	22.2
TBU	20.9	18.1	32.0
CRR	0.00	85.9	100.0

In order to improve the readability of the previous enunciated indicators, a graphical representation is presented in Figure 9, compared to the best-case scenario, from the owner of the installation, of each KPI. Given its relevance within the core of this work, for each strategy, the battery SoC evolution was compared and is presented in Figure 10.

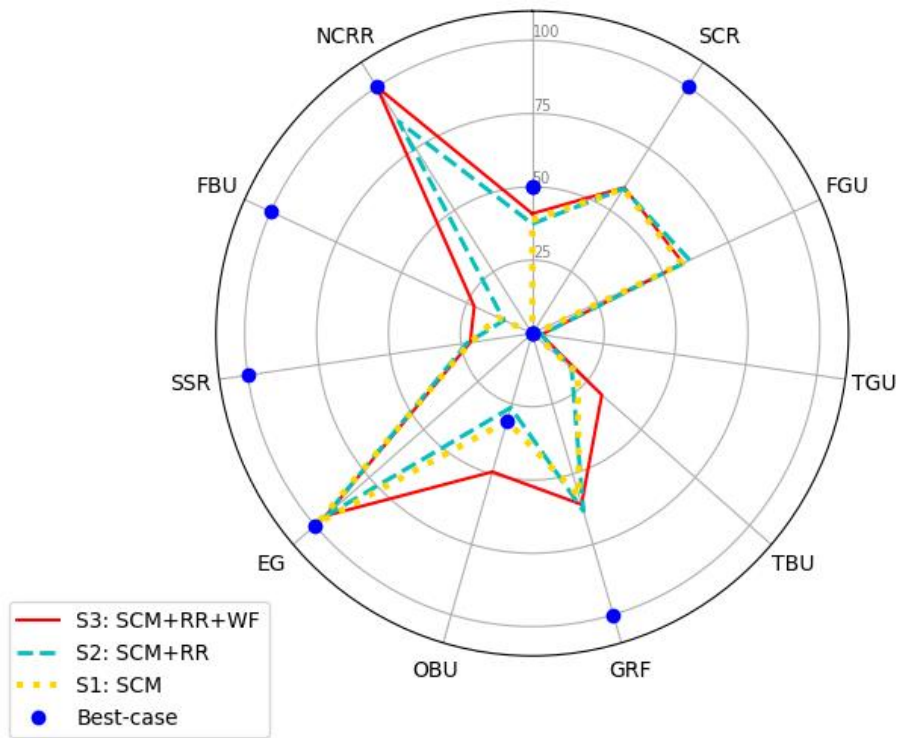


Figure 9 - KPIs representation for each of the strategies studied.

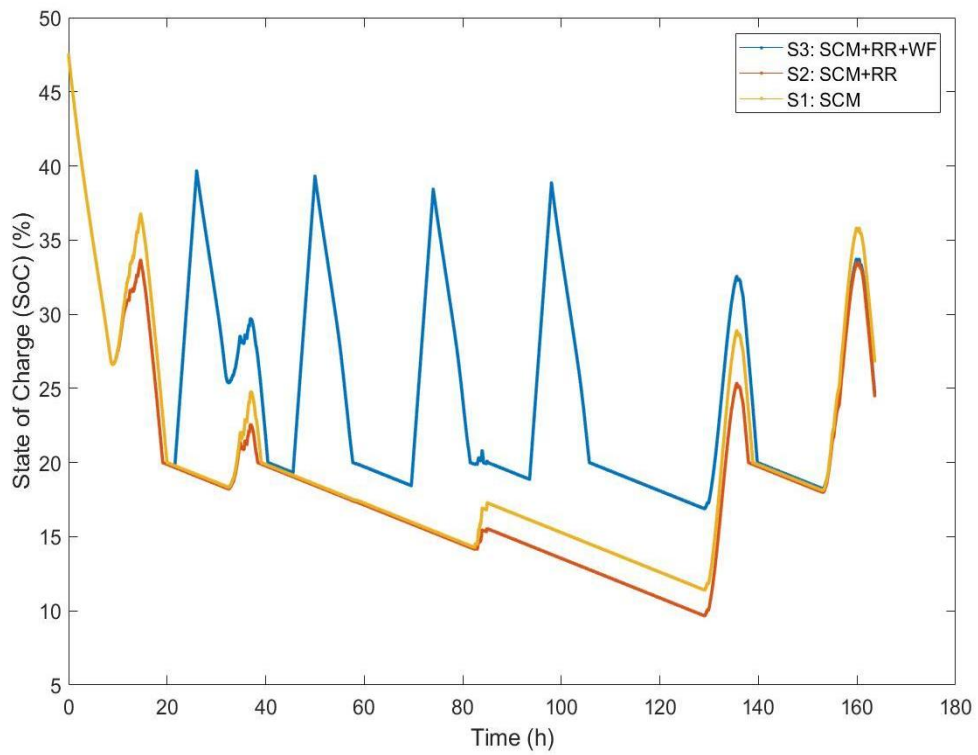


Figure 10 – Simulation of the battery SoC for the three strategies, over the same week PV-generation and load profiles.

## 5. Experimental validation with the VRFB

The real-time operation of the SCM+RR+WF (strategy 3) and experimental validation details are presented in this section. As previously referred, the study made in [11] validated the SCM (strategy 1) using the same experimental setup and battery. Strategy number 2 is a simplification of strategy number 3. Being the SCM+RR+WF (strategy 3) the most complex strategy, both on algorithm or control implementation, when compared to strategy 1 and strategy 2, it was decided to implement the SCM+RR+WF only and validate it at full scale and real operating conditions in the experimental microgrid of the VRFB. For the chosen week (1-7 January 2018), the IPMA API weather forecast was consulted for the next day forecasts, resulting in an active SoC control (night battery charge) on the day 2, 3, 4 and 5. On days 1, 6, and 7, due to the weather forecast, the active SoC control was not activated. The VRFB experimental SoC was calculated through the battery's manufacturer's curve, as explained in the work developed in [11].

The control algorithm was programmed in the LabVIEW environment (Figure A.1 – appendix) and implemented, successfully achieving a control cycle time of about 2 seconds. In Figure 11, the evolution of SoC is shown, comparing the simulation results and the experimental results of the strategy SCM+RR+WF.

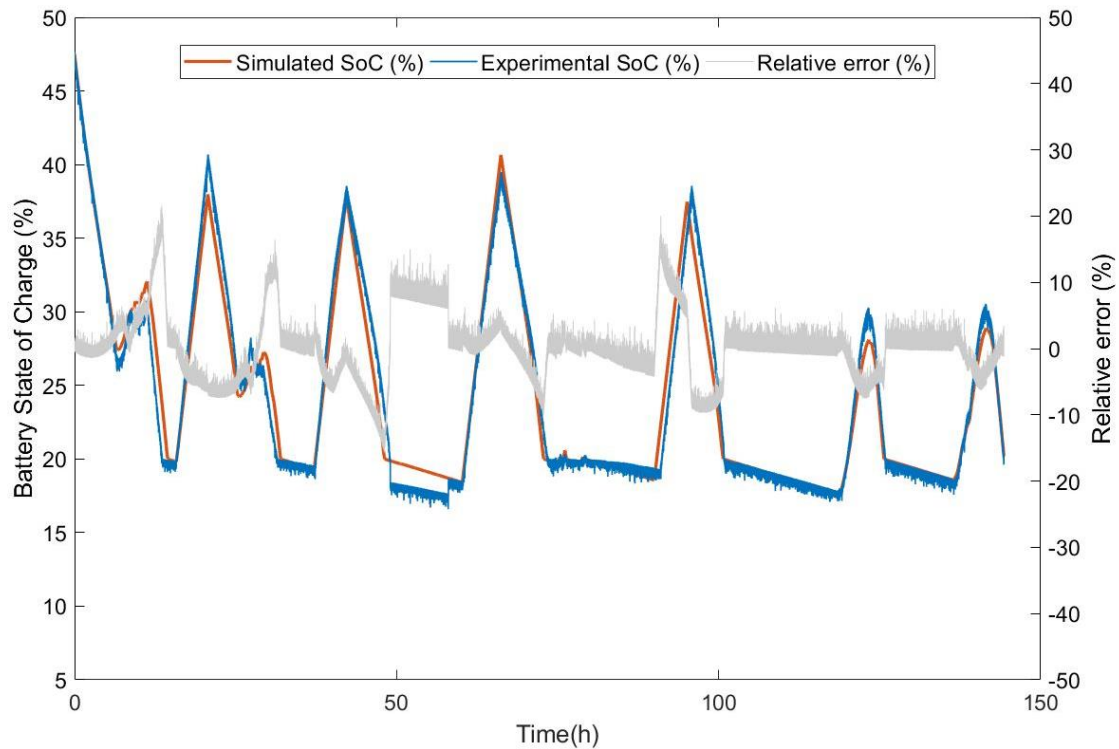


Figure 11 – SoC evolution over the week: SCM+RR+WF simulation vs real-time implementation results, with a mean absolute error of 3.5%, over the period studied.



## 6. Discussion

The analysis made concerns one week in the Portuguese winter season, a season usually characterized by several daily fluctuations in the PV power generation, and by the time of year with the lowest average daily global solar radiation. Figure 4 depicts the PV power generation over the period studied, with days characterized by high PV variability (except for day 6), posing a challenging scenario concerning power ramps.

A RR control only works properly with a battery SoC control. This control can be made differently, depending on the desired objective. In this work, a direct relationship between the battery SoC and the weather forecast was created. This approach allowed a battery SoC to be more controlled and prepared energy capacity to the next day's absorption or injection PV ramping needs. The aim of using this control type was to relate the geographical location of the PV installation, with the management of the battery. Improvements in battery forecast will impact the improvement of EMS. MA is a satisfactory method to approach the RR calculation and was satisfactorily implemented in this VRFB. MA implies more cycling number than other RR techniques, which is not an obstacle for this work since this VRFB presents a considered nominal energy capacity (60 kWh). Within the MA, the time frame has a great impact on results, as observed in Figure 5. The 20 s average time frame allowed a high number of maximum controlled ramps and is not too much affected by the averaging of several different measurements of PV generation fluctuations.

From the KPI results, it can be seen that, for all the strategies, the SCR parameter is very similar. Besides the PV-generated energy that is consumed directly by the installation, this parameter is dependent on the availability of the battery to charge or discharge. This is the main reason the strategy 2 and 3 present a slightly higher SCR than the classical approach of strategy 1. Considering the understudy week, the SCR is far from its theoretical maximum due to the PV generation of energy being greater than the global energy load profile. The relation between the PV-generation and the load profile suffers a wide variation throughout the entire year (seasonality). The energy used for ramp control tasks (PV or battery) is lower when compared with the consumption needs. This means that this objective does not greatly penalize the SCR KPI. The SSR indicator is curiously the same on strategy 1 and 3, and slightly higher than strategy 2. This indicates the RR control does not affect the consumed PV energy, which was a priority to follow within the three strategies. Given the PV-generation and load profiles, the GRF is marginally higher for strategy 2 (SCM+RR). This KPI relates the energy extracted from the grid and the energy needed to supply the load. The

night battery charging of strategy 3 could have led to the highest total energy exchanged to the grid, which did not happen. The indicator EG accounts for the energy extracted from the grid, in the overall energy exchanged with the grid. Once again, the pre-conception of definitions could foster misleading conclusions. However, the strategy with a higher EG parameter, in the overall grid use, is Strategy 1 (SCM), mainly due to a lower weekly total of energy exchanged with the grid. The TGU indicator presents a growth from the simplest to the most complex strategy, meaning an increased energy injected into the grid, although the injection of strategy 2 and 3 is controlled, since the RR control is activated whenever a violation of the RR limit occurs. The energy extracted from the grid over the load profile is represented by FGU. Strategy 2 presents the highest value since it makes less use of the battery interaction with the loads (when devoted to the RR control). For RR control, the implementation of a SoC control algorithm also causes an increase in the battery utilization rate, as expected, which can be seen in the increase of the TBU and FBU indicators. In the case of this battery technology, VRFB, this additional usage will not reduce its lifespan or increase its degradation, which could happen in other storage technologies, for example, in lithium-ion battery technology. BCR is an indicator already presented in previous studies of EMSs, which addresses the energy used to charge the battery over the total energy exchanged with the battery. In this work, the OBU balances the use of the battery, over the load profile. The SCM+RR+WF strategy, which considers the implementation of SoC control dependent on the weather forecast (and, indirectly, the potential occurrence of extreme power ramps), can successfully control all power ramps, indicated by the CRR parameter, imposing an RR limit of 10%/min. Otherwise, implementing a simple RR control strategy could only control about 86% of the total power ramps occurring in the test period.

The analysis of this work was to evaluate energy KPIs, although the importance of economic indicators is recognized. Nevertheless, it was intended to minimize the cost of charging the battery (to control SoC, when needed) overnight using the cheapest electricity tariffs (for the bi-hourly or tri-hourly tariffs).

Figure 10 presents the SoC simulation results of the three EMSs. It can be observed that the night battery charging, concerning SCM+RR+WF, occurs in the days where the PV generation is low or associated with the most variability (Figure 4). Considering the night battery charge in a mean value of 2700 W, and the PV-generation and load profiles, the battery SoC never exceeds 50 % for any strategy throughout the studied week. The implementation has associated errors among the micro-grid equipment, namely, battery

efficiency, power converters efficiency, measurement devices, computer command delay, and ethernet dependency (ethernet communication must be solid to assure quality). Considering the results of Figure 10, the difference between the simulation and the experimental output presents a low error (absolute average of 3.5 % over the period of study) when compared with the experimental validation. This fact points to a model with a good representation of the battery, with the ability to simulate the VRFB behaviour with the suited precision. Additional improvement will be carried out to further reduce the existing error.

## 7. Conclusions

In this work, a residential/services system was object of study, considering a PV installation, an electricity storage unit – a VRFB –, and a load profile over one week of wintertime, with data from January 2018. Three energy management strategies were simulated, to obtain a result improvement of the main KPIs related to the self-consumption maximization and power RR control.

Strategy 1, SCM, performs a simple self-consumption maximization of the PV power generation; strategy 2, SCM+RR, additionally performs a RR control, imposing a 10 %/min of the PV nameplate capacity RR limit, providing additional stability over the grid energy exchange. Strategy 3, SCM+RR+WF, added a 12-hour weather forecast, based on the IPMA API, to implement a SoC control, able to prepare the battery to better deal with the next-day PV power ramps. For the year 2018, and based on local data, it was shown that about 5% of the PV power ramps that occurred were above the rate of 10%/min of the PV nameplate capacity understudy. To improve confidence in this RR occurrence distribution, it is necessary to collect data from a wider period, in a similar way to a typical meteorological year. Based on the obtained results, it can be concluded that strategy 3, SCM+RR+WF, presented a good approach to perform an SoC control to accommodate the next day's ramp-rates. The night battery charging presented a simple solution to follow in the winter season, conditioned to SoC at the end of the day. It should be noted that for summertime, probably, the opposite should take place – a nightly discharge. Strategy 1 (SCM) is the EMS most known worldwide, due to its simple application and suitability to the domestic and services sectors, although it does not deal entirely with solar PV fluctuations. This issue should be carefully addressed, given the increase of solar PV installations in these areas. The first approach was to simulate the outputs of implementing the RR control, although its single use

in the domestic and services sector should be combined with another strategy. This strategy is Strategy 2 (SCM+RR), which has proven to be insufficient to control all power ramps violating the RR defined limit.

Despite the challenging scenario of occurrence of power ramps in the selected week, the SCM+RR+WF strategy demonstrated to be able to control 100% of the ramps with rates above 10%/min, without significantly reducing the PV SCR (61%), and being able to keep the GRF at 68%, successfully achieving the proposed objective of this work. An indicator exclusive for battery cycling analysis should be further addressed.

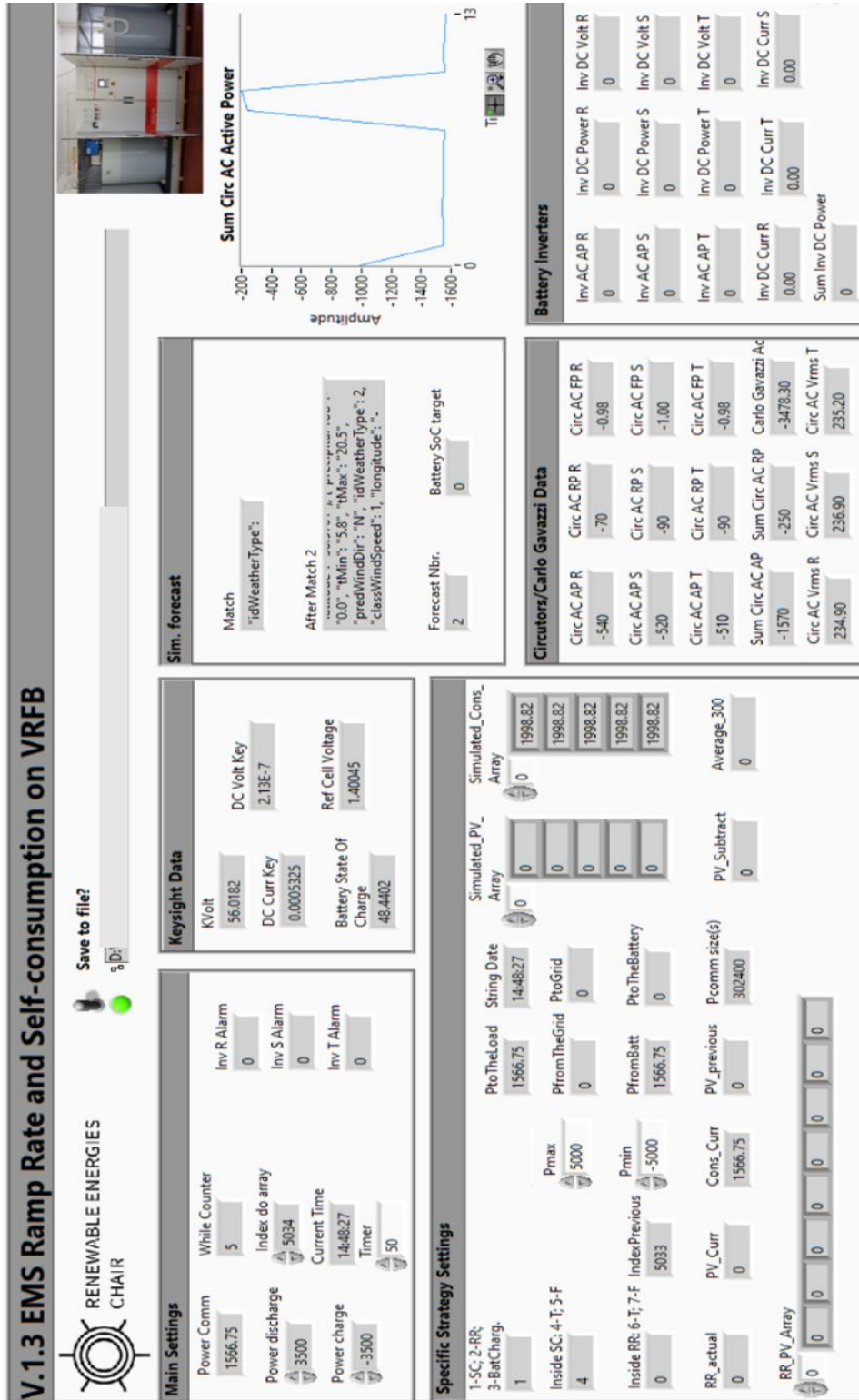
The development of multi-objective EMSs, often with competing goals such as the SCM+RR+WF, present different system needs for power, energy, usage cycles, or response time. The prosumer can thus probably benefit from the use of hybrid battery systems, combining the strengths of different technologies, which presents itself as a path for future research work.

## **Acknowledgements**

The authors would like to thank the support of this work, developed under the European POCITYF project, financed by 2020 Horizon under the grant agreement no. 864400. This work was also supported by the PhD. Scholarship (author Ana Foles) of FCT – Fundação para a Ciência e Tecnologia –, Portugal, with the reference SFRH/BD/147087/2019.

# Appendices

Figure A.1 - LabVIEW program user interface (GUI), used to implement and validate the SCM+RR+WF strategy.



## 8. References

- [1] IRENA, *Renewable Capacity Statistics 2020*. 2020.
- [2] IRENA, *Innovation landscape for a renewable-powered future: Solutions to integrate variable renewables*. 2019.
- [3] T. Ackermann, N. Martensen, T. Brown, P.-P. Schierhorn, F. G. Boshell, and M. Ayuso, “Scaling Up Variable Renewable Power: The Role of Grid Codes,” p. 106, 2016.
- [4] Q. Zheng, J. Li, X. Ai, J. Wen, and J. Fang, “Overview of grid codes for photovoltaic integration,” *2017 IEEE Conf. Energy Internet Energy Syst. Integr. EI2 2017 - Proc.*, vol. 2018-Janua, pp. 1–6, 2017.
- [5] V. Gevorgian, M. Baggu, and D. Ton, “Interconnection Requirements for Renewable Generation and Energy Storage in Island Systems: Puerto Rico Example: Preprint,” no. May, 2017.
- [6] J. Martins, S. Spataru, D. Sera, D. I. Stroe, and A. Lashab, “Comparative study of ramp-rate control algorithms for PV with energy storage systems,” *Energies*, vol. 12, no. 7, 2019.
- [7] M. G. Alvarez, Javier Marcos; Laita, Iñigo de la Parra; Palomo, Luis Marroyo; Pigueiras, Eduardo Lorenzo; Solano, “Grid integration of large-scale PV plants: dealing with power fluctuations,” *Large Scale Grid Integr. Renew. Energy Sources*, pp. 131–170, 2017.
- [8] M. M. A. Omran, Walid A.; M. Kazerani; Salama, “Investigation of Methods for Reduction of Power Fluctuations Generated From Large Grid-Connected Photovoltaic Systems,” *IEEE Trans. Energy Convers.*, vol. 26, no. 1, pp. 318–327, 2011.
- [9] I. de la Parra, J. Marcos, M. García, and L. Marroyo, “Control strategies to use the minimum energy storage requirement for PV power ramp-rate control,” *Sol. Energy*, vol. 111, pp. 332–343, 2015.
- [10] A. Ellis, D. Schoenwald, J. Hawkins, S. Willard, and B. Arellano, “PV output smoothing with energy storage,” *Conf. Rec. IEEE Photovolt. Spec. Conf.*, no. March, pp. 1523–1528, 2012.

- [11] L. Fialho, T. Fartaria, L. Narvarte, and M. C. Pereira, “Implementation and validation of a self-consumption maximization energy management strategy in a Vanadium Redox Flow BIPV demonstrator,” *Energies*, vol. 9, no. 7, 2016.
- [12] J. Moshövel *et al.*, “Analysis of the maximal possible grid relief from PV-peak-power impacts by using storage systems for increased self-consumption,” *Appl. Energy*, vol. 137, pp. 567–575, 2015.
- [13] Circutor, “No Title,” *CVM-1D Series*. [Online]. Available: <http://circutor.com/en/products/measurement-and-control/fixed-power-analyzers/power-analyzers/cvm-1d-series-detail>. [Accessed: 14-Dec-2020].
- [14] EDP Distribuição, “Atualização dos perfis de consumo, de produção e de autoconsumo para o ano de 2018 Documento Metodológico (artigo 272.º do Regulamento de Relações Comerciais),” 2018.
- [15] A. Foles, L. Fialho, M. Collares-Pereira, P. Horta, “Vanadium Redox Flow Battery Modelling and PV Self-Consumption Management Strategy Optimization,” 2020.
- [16] IPMA, “IPMA API.” [Online]. Available: <http://api.ipma.pt/open-data/forecast/meteorology/cities/daily/>.
- [17] European Centre for Medium-Range Weather Forecasts, “No Title.” [Online]. Available: <https://www.ecmwf.int/>. [Accessed: 14-Dec-2020].
- [18] National Centre for Meteorological Research, “AROME.” [Online]. Available: <https://www.umr-cnrm.fr/spip.php?article120&lang=en>. [Accessed: 14-Dec-2020].
- [19] EDP Comercial, “No Title,” *Electricity Tariffs*. [Online]. Available: <https://www.edp.pt/particulares/energia/tarifarios/>. [Accessed: 14-Dec-2020].
- [20] F. P. M. Kreuwel, W. H. Knap, L. R. Visser, W. G. J. H. M. van Sark, J. Vilà-Guerau de Arellano, and C. C. van Heerwaarden, “Analysis of high frequency photovoltaic solar energy fluctuations,” *Sol. Energy*, vol. 206, no. May, pp. 381–389, 2020.